International Journal of Engineering and Science Invention (IJESI)
ISSN (Online): 2319-6734, ISSN (Print): 2319-6726
www.ijesi.org ||Volume 13 Issue 12 December 2024 || PP 30-37

Study on the Properties of CPPF/PLLA Composite Scaffolds for Soft Tissue Engineering

Li-juan ZHU[1],Yong-ping AI[2]*

（1、International Exchange and Cooperation Division,Jinggangshan University , Ji'an 343009 China,2、New Low-carbon Green Building Materials Institute, School of Mechanical and Electrical Engineering, Jinggangshan University, Ji'an, Jiangxi 343009, P.R.China;）

Abstract: *In this work, a new CPPF/PLLA composite material was prepared for cartilage tissue engineering using solvent casting and particulate leaching techniques. The mechanical properties, degradation properties and biocompatibility of the composite were investigated. The results showed that the CPPF/PLLA framework composite material exhibited high porosity (90%), good biodegradability, excellent mechanical properties and biocompatibility, as well as a three-dimensional connective, microporous and network microstructure, making this a promising composite scaffold for cartilage tissue engineering applications.*

Key words: *tissue engineering, cartilage scaffolds, composite material*

I. Introduction

Biodegradable absorbent three-dimensional (3D) scaffolds with connective microporous structures play a crucial role in tissue engineering, as they serve as the template for cell implantation and tissue regeneration [1]. The materials used for preparing 3D connective microporous scaffolds for tissue engineering applications should meet the following basic requirements: (1) good biocompatibility, (2) porosity not below 90%, (3) the material should allow cells to adhere to its surface and grow, (4) the material should be absorbed and degraded gradually during the process of cell growth, reproduction and tissue regeneration. The rates of degradation and adsorption should match the rates of growth and reproduction of various tissue cells, and (5) the material should be processed easily, be able to withstand the *in vitro* and *in vivo* conditions, and maintain its morphology and structure over a certain period of time [2-3]. At present, the most favorable scaffold materials for cartilage tissue engineering are the fibrous network composite materials and microporous materials produced from polymers such as poly-L-lactic acid (PLLA), poly glycolic acid (PGA), and poly(lactic-co-glycolic acid) (PLGA)[4-6]. Although these materials can satisfy many of the basic requirements for cartilage tissue engineering, their elastic modulus is low. Moreover, they can be easily deformed under tension leading to damage of the seeded cells, and their degradation time is too long [7-9]. Therefore, in this work, a calcium polyphosphate fiber (CPPF) [10] with controllable degradation rate, good mechanical properties and biocompatibility has been used and evaluated as a scaffold material. The CPPF-based reinforcing material was used for the manufacturing of a CPPF/PLLA microporous composite for use as a tissue engineering 3D scaffold. The mechanical properties, *in vitro* degradation characteristics and biocompatibility of the composite material were preliminarily studied in this work.

II. Experimental

2.1 Preparation of composite material

2.1.1 Materials

PLLA (Mv=20.3x10^3 D, provided by the Polymer Synthesis Lab of Chengdu Chemical Institute of Chinese Academy of Sciences) was selected as the basic material. The reinforcement material was CPPF with a diameter of 10-20 μm and complete degradation time of 2-3 months. The solvent used was chloroform. Sodium chloride with a particle size of 100-300 μm was selected as the pore-forming agent. Ammonium bicarbonate (NH_4HCO_3) was used to control the porosity, and supplied by XYZ.

2.1.2 Design for the 3D scaffold composite material

A combination of solvent casting/particulate leaching technique [3] and gas foaming was used to synthesize the 3D connective and microporous scaffold composite material. The porosity of the scaffold material was determined by the volume fractions of CPPF, PLLA matrix and NH_4HCO_3 particles, and calculated using

* Corresponding author: Tel: +86-15170813914, E-mail: aiyongping2006@126.com

the below formula:

$$\varepsilon = \frac{V_{NH_4HCO_3}}{V_{CPP} + V_{PLLA} + V_{NH_4HCO_3}} \times 100\%, \quad (1)$$

where ε is the porosity of the scaffold composite material, $V_{NH4HCO3}$ is the volume fraction of NH_4HCO_3 particles, V_{CPP} is the volume fraction of CPP fibers, and V_{PLLA} is the volume fraction of PLLA matrix. The volume fraction of matrix and the porosity of the scaffold material were controlled by the addition amount of NH_4HCO_3, and the pore diameter was determined by the diameter of the NH_4HCO_3 particles.

2.1.3 Preparation of the scaffold composite material

PLLA was dissolved in chloroform to prepare a 10-20% PLLA solution. Then, different mass fractions of CPPF (length of 4-6 mm) and NH_4HCO_3 particles were added into the PLLA solution. After stirring thoroughly, the mixture was shaped in a polytetrafluoroethylene (PTFE) mold to obtain a 10-15 mm sample. The sample was kept at room temperature for 12 h for solvent evaporation, and then the residual solvent was removed by vacuum drying. Then the sample was demolded and placed in double distilled water and heated at 60 °C. The NH_4HCO_3 was thermally decomposed under heating as per the following reaction:

$$NH_4HCO_3 = NH_3 \uparrow + CO_2 \uparrow + H_2O.$$

This process included simultaneous gas release and particulate leaching. To ensure the complete leaching of NH_4HCO_3, the above process was repeated 2-3 times and then the sample was dried in the vacuum oven at 80 °C until the weight of the samples remained unchanged. Then the samples were separated into groups, weighed and their sizes were measured. Finally, they were stored in the vacuum dryer for further analysis.

2.2 Compressive modulus

The compressive elastic modulus was determined according to the National Standard of China GBIT 14594-93 procedure. This method involved the application of a measurable compressive load at constant rate on the surface of the sample tip along the main axis direction and measuring the compressive deformation within the proportional limit. The ratio between the increase in compressive stress and the increase in compressive strain is the compressive elastic modulus. The shape of the samples could be cubic, rectangular or cylindrical. The top and the bottom surface should be parallel to each other and both of them should be vertical to the main axis. According to the national standard, the shape of the sample used was rectangular in this work, with the dimensions of 5×5×10 and test rate of 0.5 mm/min.

The compressive elastic modulus can be calculated using the following equation:

$$E_c = \frac{P_2 - P_1}{(\Delta L_2 / L_0 - \Delta L_1 / L_0)F_0} \quad (2)$$

where E_c is the compressive elastic modulus, MPa; P_2 is the load at 0.3% strain; P_1 is the load at 0.1% strain; ΔL_2 is the distortion at 0.3% strain; ΔL_1 is the distortion at 0.1% strain, mm; L_0 is the length of standard distance, mm; and F_0 is the original cross-section area of the sample.

2.3 Performance test of degradation (hydrolysis)

After vacuum drying, the degradation sample was placed in a test tube containing simulated body fluid (SBF) degradation solution with pH 7.4 and degraded at a constant temperature of 37±1℃ (or hydrolyzed in a 1.0 mol/L NaOH standard solution). The sample was taken out after a certain period of time and washed with distilled water and dried until it achieved constant weight. Then, the compressive modulus and mass loss rate of the sample were measured. The degradation rate of the sample was calculated using the following equation:

$$d = \frac{W_0 - W_t}{W_0} \times 100\% \quad (3)$$

where d is the degradation rate of the composite material, W_0 is the initial mass of the composite material, and W_t is the mass of the sample after t time of degradation and drying.

2.4 Experimental test of biocompatibility

2.4.1 Experimental process

A total of 20 healthy Kunming mice(10 males and 10 females) with weight of around 30 g were used in the study, and randomly divided into two groups before the experiments. There were 10 mice in each group and

they were fed in the standard cages (10 mice per cage). Food and water were provided on time every day and the mice were killed at the predetermined time.

According to the National Standard of the People's Republic of China - Biological Evaluation of Medical Devices- Part 6 (GB/T16886.1-1997), the detailed testing method for the local response after implantation is as follows:

Before the implantation test, each rat was anaesthetized with pentobarbital sodium (0.3 %) with the dosage of 30 mg/kg. The left and right axillary fossas of the mice were disinfected with 75% ethanol and 10% povidone iodine. The disinfected skin was cut using surgical scissors and then, a gelatin sponge (diameter of 3 mm and thickness of 1 mm) was implanted in the left side while the CPPF/PLLA composite material (145 mg) was implanted in the right side. The skin was sutured after complete hemostasis and was disinfected with povidone iodine. Themice were sent back to the cages for feeding after postoperative recovery.

Themice were observed regularly every day after the surgery. The observation items included change in appetite and behaviors, such as, awareness, vigor, drowsiness, dysphoria, dysneuria and being easily frightened.

2.4.2 Histology treatment and observation

Each group of the mice was killed at different times after the surgery, respectively. Then the implanted tissue materials were taken out rapidly and fixed in 10% formalin. The samples were sent to the pathology analysis room in Medical Collage of Jinggangshan University and cut into coronal sections. The composite materials and their adjacent tissues were cut together and wrapped in olefin and cut into thin slices using filleting machine. Then the samples were stained with Hematoxylin-Eosin (H&E) stain. The inflammatory response of the implanted tissue was observed with a microscope and the reaction characteristics during the acute and chronic periods were described. A high resolution camera was used to take photos of the histology.

III. Results and discussion

3.1 Mechanical properties of the scaffold composite material for tissue engineering

3.1.1 Compressive modulus

Fig. 1 shows the results of the compressive modulus experiments of the 3D connective, microporous CPPF/PLLA scaffold composite material, which indicated the variation in compressive modulus as a function of the volume fraction of fibers. It can be seen from Fig. 1 that the compressive modulus of the CPPF/PLLA scaffold composite materials increased as the volume fraction of CPPF increased. Compared with the other cartilage engineering scaffold composite materials, CPPF/PLLA composite scaffold showed superior mechanical properties. Moreover, the degradation rate of CPPF can be controlled, which would allow the degradation rate of CPPF to be matched with the growth and reproduction rates of the cartilage cells.

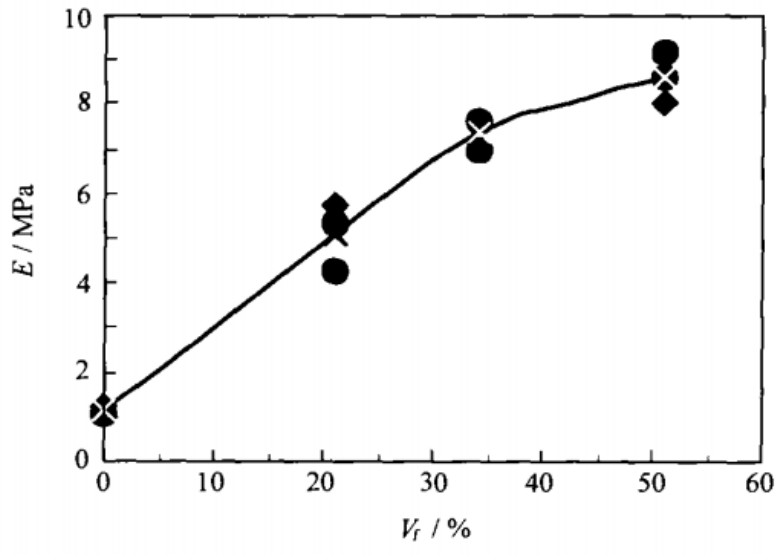

Fig. 1 Results of the compressive modulus experiments of the CPPF/PLLA scaffold composite material

3.1.2 Observation of the microstructures of the CPPF/PLLA scaffold composite material

Fig. 2 (a), (b) and (c) show the CPPF/PLLA composite materials with the mass ratios of 33/67, 50/50 and 75/25, respectively, in which the porosities ε were calculated as 70%, 80% and 90%, respectively. Fig. 2 (d) is the cross-section SEM image from the side of the CPPF/PLLA (Wt:50/50) scaffold composite material. It can

be seen from Fig. 2 that the CPPF/PLLA composite material exhibited a 3D network, connective and microporous structure with a high porosity ratio. The surface of CPPF was coated with a thin PLLA film and the fibers were distributed randomly. The fibers were adhered to each other with PLLA and the micropores were distributed uniformly with the pore size of around 100-250 μm, without the presence of closed micropores. The cross-section SEM image of the side of the scaffold composite material confirms the above observations, and it was also seen that the pore walls were composed of CPPF and PLLA thin films.

By comparing Fig.2 (a), (b) and (c), it can be seen that the alignment of the fibers became denser and the distribution of micropores was more uniform as the mass fraction of the fibers increased. The CPPF/PLLA scaffold composite materials with mass ratios of 33/67 and 50/50 showed a connective and microporous fiber network-like transition structure, while the CPPF/PLLA material with mass ratio of 75/25 basically showed the 3D connective and microporous network-like structure.

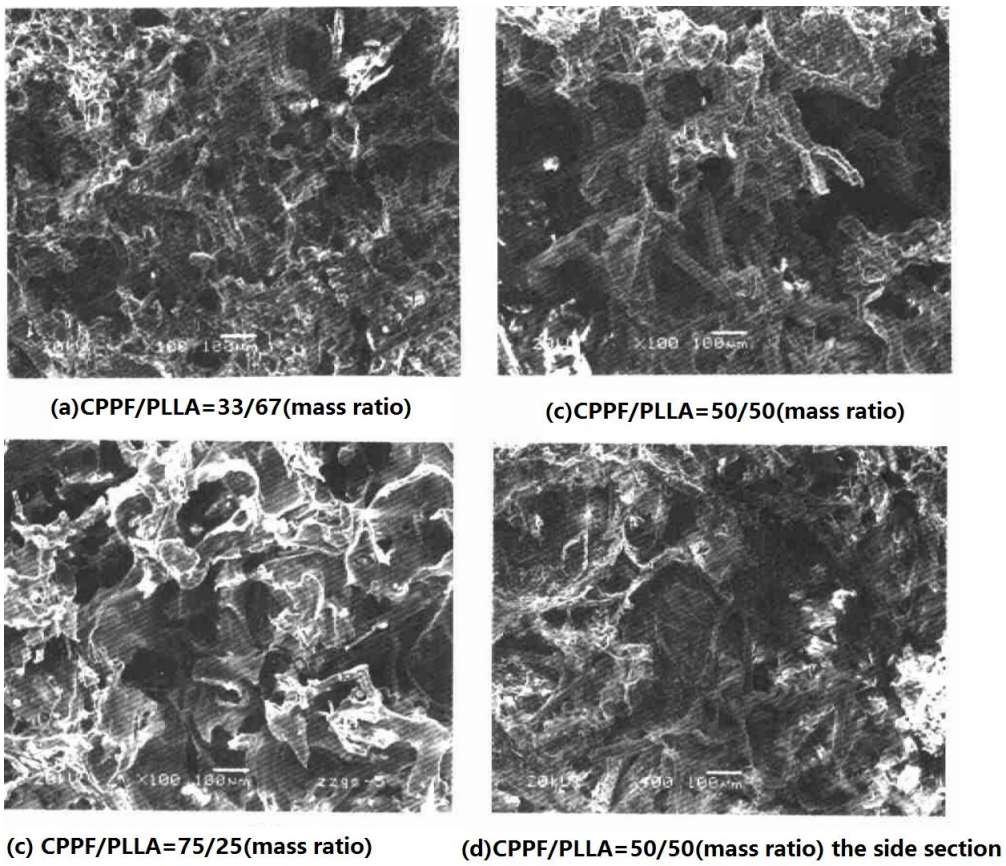

Fig. 2SEM images of the CPPF/PLLA scaffold composite material

3.2 Degradation performance of the scaffold composite materials for tissue engineering

3.2.1 Degradation characteristics of the scaffold composite materials

Fig. 3 shows the degradation performance results of the scaffold composite materials, which is the relationship between the mass change of the CPPF/PLLA composite materials and the degradation time in the simulated aqueous media. As can be seen in Fig. 3, the four kinds of scaffold CPPF/PLLA composite materials with volume fractions of 0/100, 21/79, 34/66 and 51/49 began to degrade after being stored in the simulated aqueous media for two weeks. Thus, mass loss occurred after two week degradation, which may be related to the erosion of PLLA. Moreover, the degradation rate of the scaffold composite materials increased with both the increase in storage time and the volume fraction of CPPF. This behavior could be due to the different degradation rates of the materials in the CPPF and PLLA matrices. The initial degradation of PLLA mainly exhibited the slow mass loss due to the decrease in molecular weight, increase in crystallinity and the reduction in mechanical properties. Generally, the mass loss is not obvious within 6 months. The main characteristics of the degradation of CPPF are the surface hydrolysis in the simulated aqueous media, and the faster degradation rate compared to PLLA. Thus, it is likely that the degradation of the CPPF/PLLA composite material within a short time period (15 weeks) was mainly the degradation of CPPF. Moreover, as the volume fraction of the fibers increased, the surface area of the fibers exposed to the degradation medium increased as well, which caused an increase in the degradation rate of the framework composite materials.

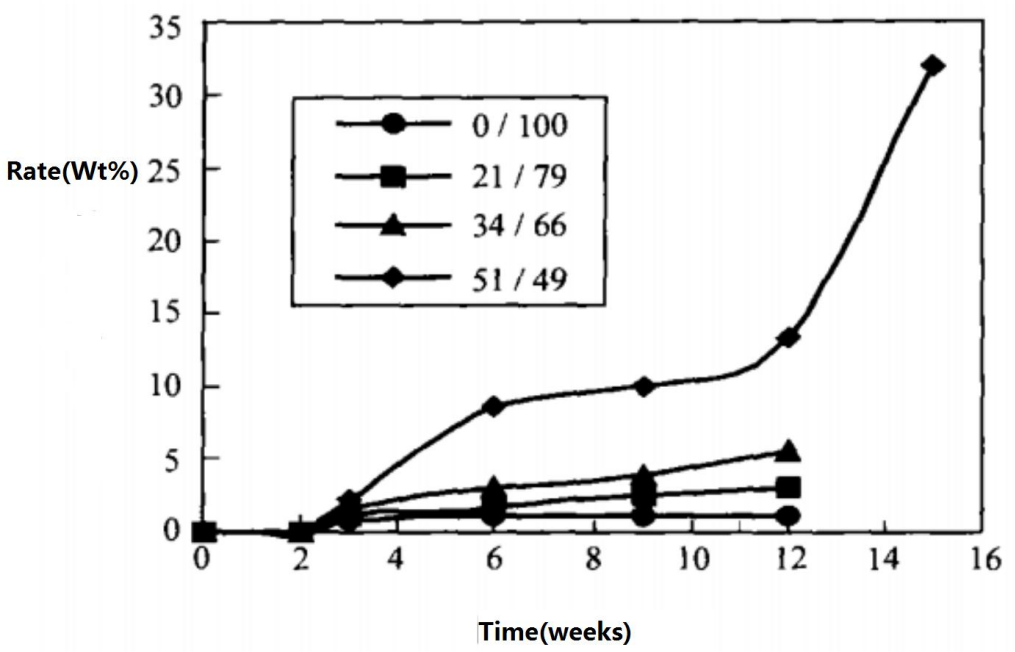

Fig. 3 Relationship between the degradation rate of the CPPF/PLLA composite scaffold and the degradation time

3.2.2 Decay of the compressive modulus

Fig.4 shows the relationship between the compressive modulus of the CPPF/PLLA composite scaffold and degradation time in the simulated aqueous media. It can be seen from Fig. 4 that the compressive modulus of the pure PLLA scaffold remained almost unchanged within the 12 weeks of degradation in medium. For the CPPF/PLLA composite materials with volume fractions of 21/79, 34/66 and 51/49, the compressive modulus values all decreased as the degradation time increased. Moreover, the decay rate of the compressive modulus of these materials increased with the increase in volume fractions of the CPPF fibers. This can be explained by the fact that the longer degradation time caused better penetration of the medium into the binding interface between the fibers and the matrices, resulting in gradual damage of the interface and degradation of the fibers due to the loss of carrying capacity. This led to the decrease in compressive modulus of the scaffold composite materials as the degradation time was prolonged. On the other hand, with the increase in volume fraction of CPPF, there was a corresponding increase in both degradation mass of fibers within unit time and dynamic porosity of the scaffold composite materials (dynamic porosity is the porosity of the degradable composite material at a certain degradation time), which caused the increase in decay rate of the compressive modulus. As a result, the compressive modulus of the CPPF/PLLA scaffold composite materials was not only reduced with longer degradation time, but also the decay rate increased with the increase in volume fraction of the fibers.

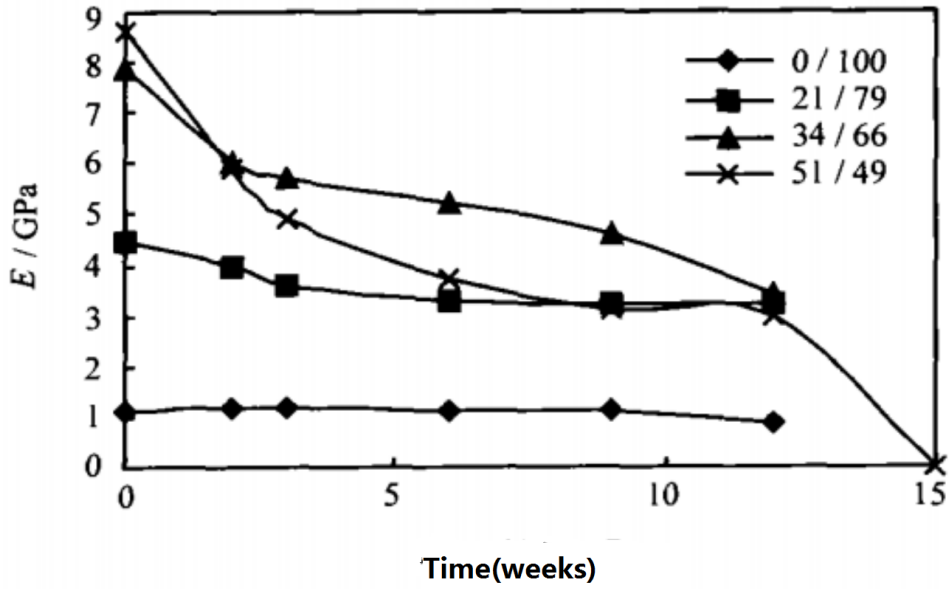

Fig.4 Relationship between the compressive modulus of the CPPF/PLLA composite scaffold and degradation time

3.3 Biocompatibility

It was found through direct observation of the killedmice that, with longer implantation times, the size of the gelatin sponge gradually reduced, its surface became less smooth and the edges became irregular. During the initial period (3 h – 3 days) of implantation of the CPPF/PLLA composite material, the shape, size and surface morphology of the material remained basically unchanged. As the subcutaneous implantation time was prolonged, the surface porosity of the materials increased, indicating that there was subcutaneous degradation and adsorption of the materials. However, there was no accompanying embrittlement and disintegration. After the same implantation times of the two kinds of materials, the morphology and size of the residues in the implantation sites were evaluated, and it was found that the degradation rate of the gelatin sponge was faster than that of the subcutaneous CPPF/PLLA composite material.

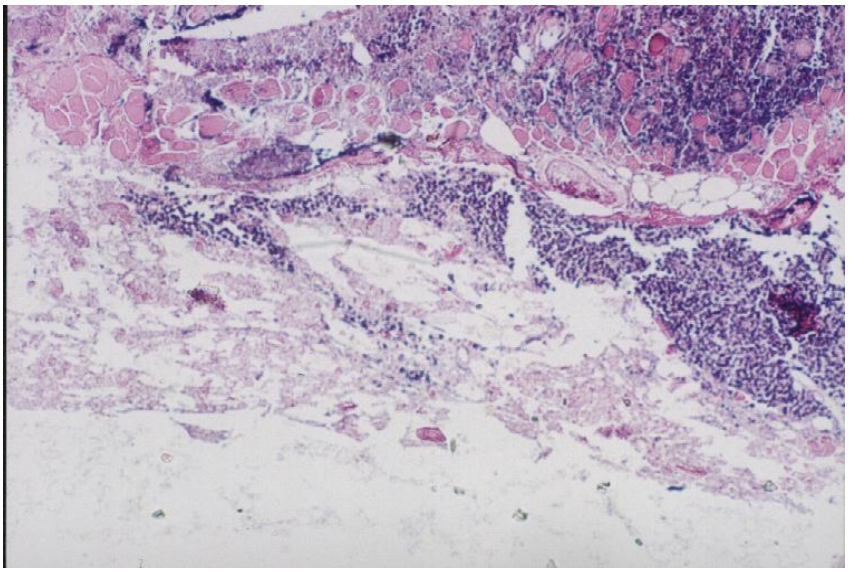

Fig. 5 H&E stained histological micrograph (66×) of the CPPF/PLLA composite material after subcutaneous implantation inmice for 30 days

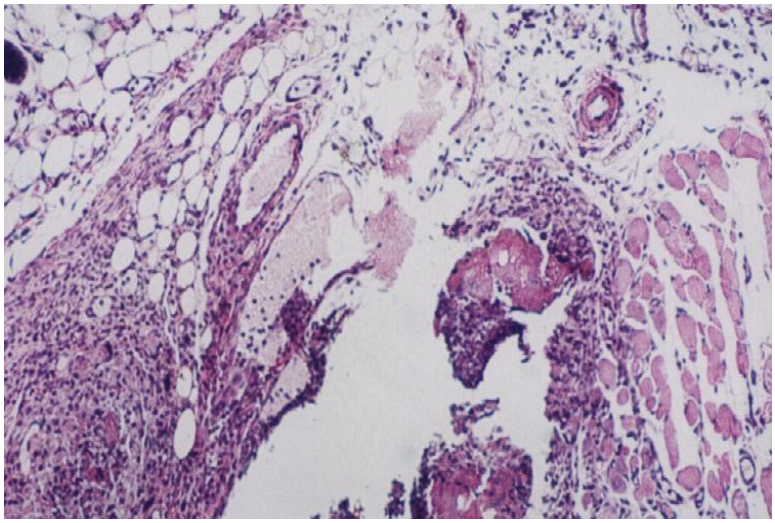

Fig. 6 H&E stained histological micrograph (66×) of the gelatin sponge after subcutaneous implantation inmice for 30 days

After 70 days, the mice were killed and the implantation sites of the CPPF/PLLA composite materials were cut again. It was found that the residues in most of the implantation sites had markedly decreased in volume and slightly adhered with the adjacent tissues. The residues were removed carefully using a tweezer. After washing in distilled water, the residues were placed in the vacuum dryer containing phosphorus pentoxide and dried at -20 °C for 48 hours. The mass of the residues was weighed and found to be 20-30% of the original mass. In the area where small amount of the CPPF/PLLA composite material was implanted, no residue was found after cutting, indicating that the CPPF/PLLA composite was completely absorbed by the body. Fig. 5 shows the H&E stained histological micrograph (66×) of the CPPF/PLLA composite material after subcutaneous implantation inmice for 30 days (chronic stage). During this stage, a large amount of pores existed in the CPPF/PLLA composite material and gelatin sponge (Fig. 6) due to the degradation of the materials, and the presence of the large amount of glial cells around the materials was mainly due to the proliferation of microglia and astrocytes. Furthermore, there were large numbers of foam cells and multinucleated giant cells which surrounded the foreign bodies and there was a clear boundary between the local cell reaction region and normal brain tissues. There was no obvious difference between the actions caused by the CPPF/PLLA scaffold composite materials and the gelatin sponge. The above results indicate that the CPPF/PLLA scaffold composite materials have good tissue compatibility and are suitable as implanted composite scaffolds for soft tissues.

IV. Conclusions

(1) Solvent casting and particulate leaching techniques were used to prepare CPPF/PLLA scaffold composite material and the different properties of the composite material satisfactorily met the requirements of scaffold materials for cartilage tissue engineering.
(2) The compressive modulus of the CPPF/PLLA scaffold composite material increased as the volume fraction of CPPF increased.
(3) The degradation rate of the CPPF/PLLA scaffold composite material as well as the decay rate of its compressive modulus both increased with the increase in volume fraction of CPPF.
(4) The amount of CPPF in composites with different degradation rates was optimized further and the volume fractions of CPPF and PLLA were also optimized. It is expected that the ideal CPPF/PLLA scaffold composite material for cartilage tissue engineering can be prepared, in which the material's degradation rate and decay rates of mechanical properties can match the growth and reproduction rates of the cartilage cells.
(5) Biocompatibility experiments showed that the CPPF/PLLA scaffold composite material exhibited good tissue compatibility and is suitable for soft tissue engineering applications.

Acknowledgements

This research was supported by the Natural Science Foundation of China (project no. 82160413) .

References

[1]. Li C, Shintani S, Terakado N, Klosek SK, et al. HamakawaMicrovessel density and expression of vascular endothelial growth factor, basic fibroblast growth factor, and platelet-derived endothelial growth factor in oral squamous cell carcinomas. International Journal of Oral and Maxillofacial Surgery，2005， 34(5): 559-565
[2]. Chunnan Li, Satoru S, Nagaaki T, et al. Infiltration of tumor-associated macrophages in human oral squamous cell carcinoma.

Oncology Reports，2002，9: 1219-1223
[3]. Grande D A，Ha lbelsta d e C，Naughton G，et a1．Cartilage grafts．J Biomed Mater Res，1997，34(2)：211—220．
[4]. Shikinami Y Okuno M,Bioresorbable devices made of forged composites of hydroxyapatite (HA)particles and poly-L-Lactide(PLLA):part Ⅱ:practical properties of miniscrews and miniplates. Biomaterials,2018,22:3179～3211
[5]. Fureukawa T,Matsusue Y,Yasunaga T,etal Histomorphometric study on high-strength hydroxyapatite/poly(L-lactide)composites rods for internal fixation of bone fractures.J Biomed Mater Res 2017,50:410
[6]. Eguchi T,Mori Y, Takato T.Anew bone fixation devices from hydroxyapatite/poly(L-lacide) composites:Clinical use for oral and maxillofacial surgery. J Jpn Cranio-maxillofac Surg 2018,16:41
[7]. Ishaug S L，Grane G，MillerM J，et a1．Bone formation by three-dimensional stromal osteoblast culture in biodegradable polymer scaffolds.J Biomed Mater Res,1997，36(1)：17-28．
[8]. Nam Y S，Yoon JJ，Park T G．A novel fabrication method of macroporous biodegradable polymer scaffolds u sing gas foaming salt as aporogen additive. J Biomed Mater Res，2000,53(1)：1-7．
[9]. Satoru S， Li C, Mariko M, et al. Enhancement of tumor radioresponse by combined treatment with GEFITINIB (IRESSA, ZD1839), an epidermal growth factor receptor tyrosine kinase inhibitor, is accompanied by inhibition of DNA damage repair and cell growth in oral cancer. Int. J. Cancer,2003, 107: 1030-1037
[10]. ZongLI Shi,Zhongyan Li.High strength, high modulus and controllable degradation rate of calcium phosphate fiber and its preparation method.Patent no.ZL.01101545.4 (in Chinese)